Smart Shoe Based on Battery-Free Bluetooth Low Energy Sensor

Thanh Hung Nguyen, Minh Ngoc Tran, Quang Huy Le, Thi Anh Vu, Quoc Cuong Nguyen, Dai Duong Nguyen(✉), and Minh Thuy Le(✉)

Department of Instrument and Industrial Informatics (3I), School of Electrical Engineering, Hanoi University of Science and Technology, Hanoi 100000, Vietnam
{duong.nguyendai,thuy.leminh}@hust.edu.vn

Abstract. In this work, we propose a smart shoe integrated with a very-low power wireless sensor node operating in Bluetooth Low Energy (BLE) 5.0 standard. The sensor node consists of a miniaturized printed inverted-F antenna, an accelerometer and a gyroscope being placed at the bottom of the shoe to measure footstep-length, running speed and foot landing angle. The maximum power consumption of the sensor is 11 mW and it is sustained by a triboeletric nanogenerator (TENG) which generates power from the friction causing by user's motion itself and an energy storage circuit. The triboelectric energy harvester, having the size of 6 cm × 6 cm, is made of multiple pairs of triboelectric materials can harvest up to 32 mW/m^2, enough to supply the sensor node.

Keywords: Smart shoe · Battery-less wireless sensor · BLE sensor · Triboelectric · Energy harvesting · Printed inverted-F antenna

1 Introduction

With the rapid development of big data, wireless sensors are becoming more and more important in data collecting. Wireless sensor nodes are useful thank to their mobility, independent operation, compactness, and interconnection, suitable to various measuring objects. Recently, many applications are being developed based on wireless sensors such as health monitoring, security or smart home. Currently, the majority of wireless sensors are being supplied by battery. However, due to the limited lifespan, they are not sustainable. Instead, other solutions must be made to increase the using time while reducing the number of batteries needed. Harvesting energy from the environment is a potential candidate to replace, or at least support, the batteries as primary power source for low power wireless sensor nodes. Among various power sources available in the ambience, triboelectricity-the phenomenon in which electricity is generated from mechanical friction, proves to be a suitable option for wearable sensors. Earlier works have succeeded in collecting from 3.2 mW/m^2 up to 313 mW/m^2 [1], showing vast potential of this energy source. In this paper, we propose the design of a smart shoe integrated with a wireless sensor node, which in turn being powered in part by triboelectricity. The sensor node,

N.-S. Vo et al. (Eds.): INISCOM 2021, LNICST 379, pp. 156–166, 2021.
https://doi.org/10.1007/978-3-030-77424-0_13

with the size of 4.5 cm × 3 cm, consumes 11 mW at maximum, measures the running speed, step, landing angle, then transmits the information using BLE technology. The triboelectric generator, with the size of 5 cm × 5 cm is able to harvest up to 32 mW/m^2, correspond with 12 µJ for each footstep.

2 System Design

2.1 The Proposed Smart Shoe

The block function of the entire system integrated on the shoe is shown in Fig. 1. Three main functional blocks are: the triboelectric based energy harvesting and storafe, the sensors, and the BLE transceiver, in which the sensors and transceiver consume 11 mW in their normal operating mode.

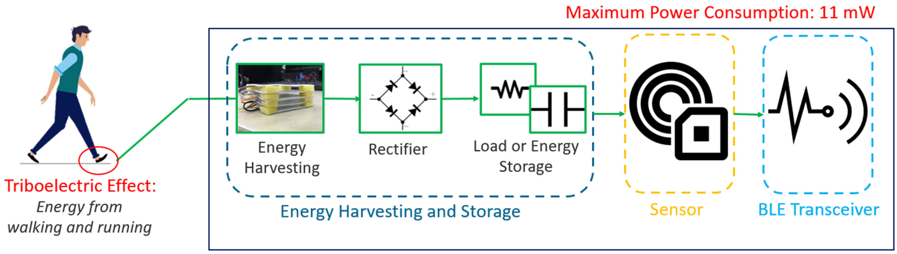

Fig. 1. Block diagram of the smart shoe.

The position of three main functional blocks on the shoe is depicted in Fig. 2, including the triboelectric nanogenerator, the energy harvesting and storage, and the BLE wireless sensor. These positions must be anaylsed to achieve maximum performance in term of the harvested power and power supply, the BLE antenna efficiency and the distance of communication of the BLE sensor.

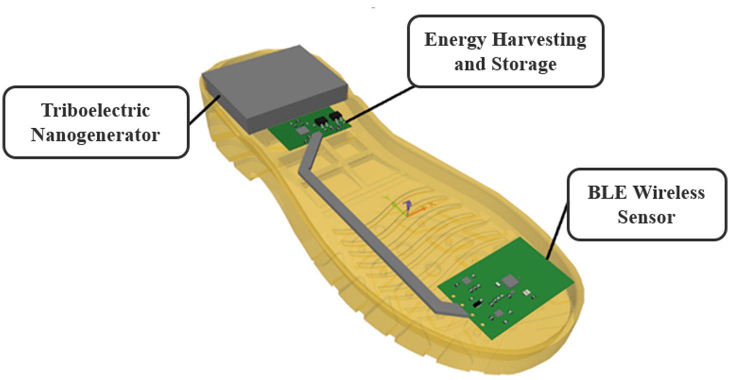

Fig. 2. The position of three functional blocks on the shoe.

2.2 Proposed Self-powered BLE Sensor

From the need of of runners, the parameters to be measured include running speed, the number of steps over time, the step length. The main criterion set for the smart shoe are shown in Table 1:

Table 1. The measured parameters, their ranges and the desired error.

Parameters	Range	Unit	Error (%)
Speed	$0 \div 12.5$	m/s	$5 \div 10$
Stepping rate	$0 \div 300$	Step/minute	$5 \div 10$
Step length	$0 \div 2.7$	M	$5 \div 10$
Landing angle	$0 \div 90$	Degrees	$5 \div 10$

In order to measure the above parameters, accelerometers (for speed, step length and stepping rate) and gyroscopes (for landing angle) are selected and listed in Table 2 (Fig. 3).

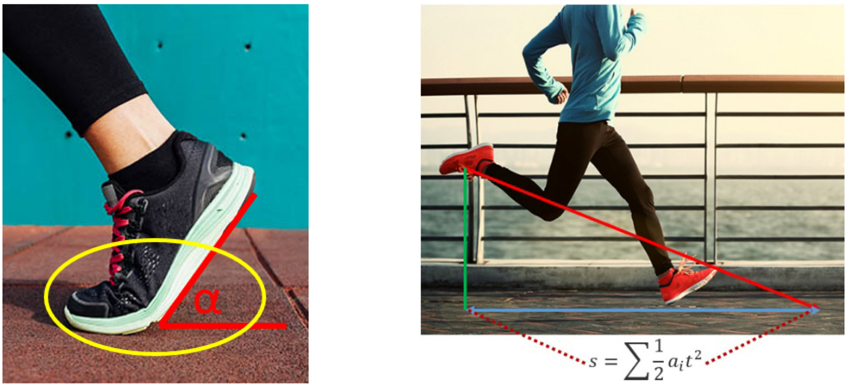

(a) (b)

Fig. 3. The measured parameters of the BLE sensor node (a) foot landing angle and (b) speed, length and stepping rate.

The DA14585 wireless transceiver operates with BLE standard and has its power consumption provided in [2]. The power consumption in various operatin modes of the BLE transceiver is listed in Table 3:

Table 2. List of the selected devices.

Device	Selected model	Power consumption
Wireless transceiver	DA14585	11 mW
Accelerometer	MMA8451Q	10.8 uW
Gyroscope	BMG250	1.53 mW

Table 3. Power consumption in various operating modes of the BLE transceiver.

Device	Power consumption
Power-down Mode	1.56 uW
Sleep-mode (@retain 16 kB RAM)	3.6 uW
TX mode (@ 0dBm)	10.2 mW
RX mode (@ 1Mbps)	11 mW

When design the sensor node, the integration of antenna is a crucial step that determines the quality of BLE communication between the node and other BLE devices. We evaluate the printed inverted-F antenna via two main criterias: radiation pattern and reflection coefficient S_{11}. Here the miniaturized IFA antenna is designed, with the dimensions shown in Table 4 (Fig. 4).

Table 4. Dimensions of the IFA antenna (unit: mm)

Parameters	Value
w_s	2
w	0.8
L_f	5
L_1	2.8
L_2	2.2
L_3	1.7
L_4	2
L_5	3.7

When the antenna is integrated on-board, the impact of the wires and lumped elements within the circuit, and the fact that the ground is heavily mutilated due to the introduction of the lumped components make the antenna's impedance deviates and thus shift the resonant frequency significantly. The parameter L_5 of 3.3 mm is reoptimized to change the frequency back to the desired value between 2.4 GHz and 2.5 GHz

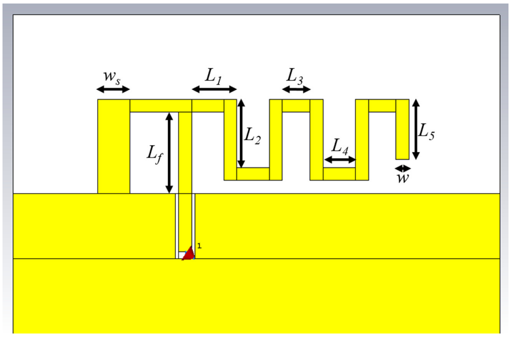

Fig. 4. The proposed miniaturized IFA antenna.

for BLE communication. As seen from Fig. 5, the antenna bandwidth and radiation pattern is still maintained after being placed inside the circuit. The antenna gain remains stable around 1.6 dBi.

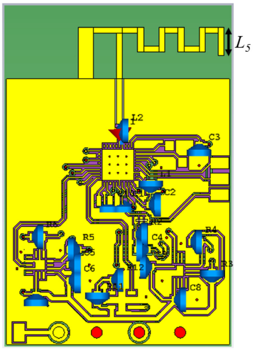

(a)

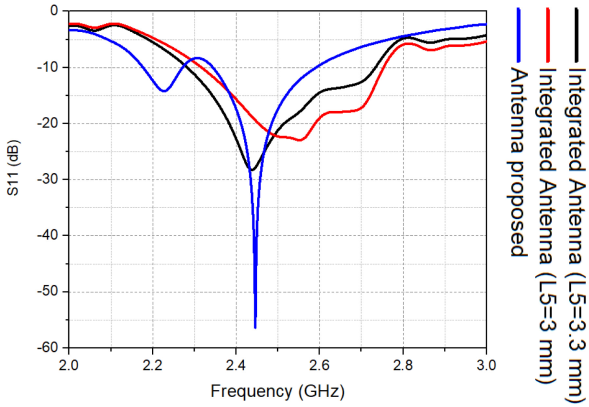

b)

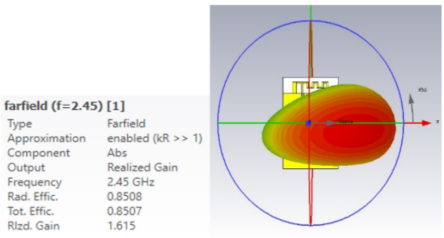

(c)

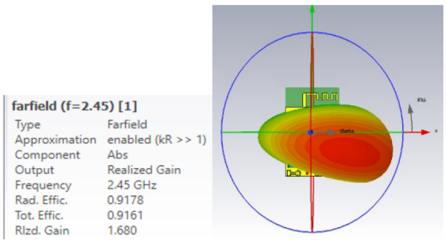

(d)

Fig. 5. (a) The layout of BLE sensor with integrated antenna, (b) the simulated S_{11} of the antenna standing alone and integrated in the BLE circuit, (c) the simulated radiation pattern of the standing alone antenna, and (d) the simulated radiation pattern of the antenna on-board.

The BLE sensor node is placed inside the shoes as we mentioned above, the influence of the shoes to antenna performance is considered, which is unveiled in Fig. 6a. The BLE sensor with integrated antenna is placed at three position: a) near the sole, b) near the arch and c) near the heel, corresponding with Fig. 6 a, b and c. If the antenna is close to the sole, the S_{11} of the antenna is slightly under -10 dB while reflection coefficients in two others positions are only under -7 dB in desired frequency.

When the heterogeneous environments are taken into account, the simulation of radiation pattern of the antenna on the BLE sensor placed near the sole is similar to the radiation pattern as in Fig. 5d but the peak gain is decreased from 1.6 dBi to 0.9 dBi. However, at two positions near the arch and near the heel the radiation pattern of the integrated antenna are not similar to the radiation pattern as in Fig. 5d as illustrated in Fig. 7. Therefore, the position near the sole is choosen to place BLE sensor node on the smart shoe.

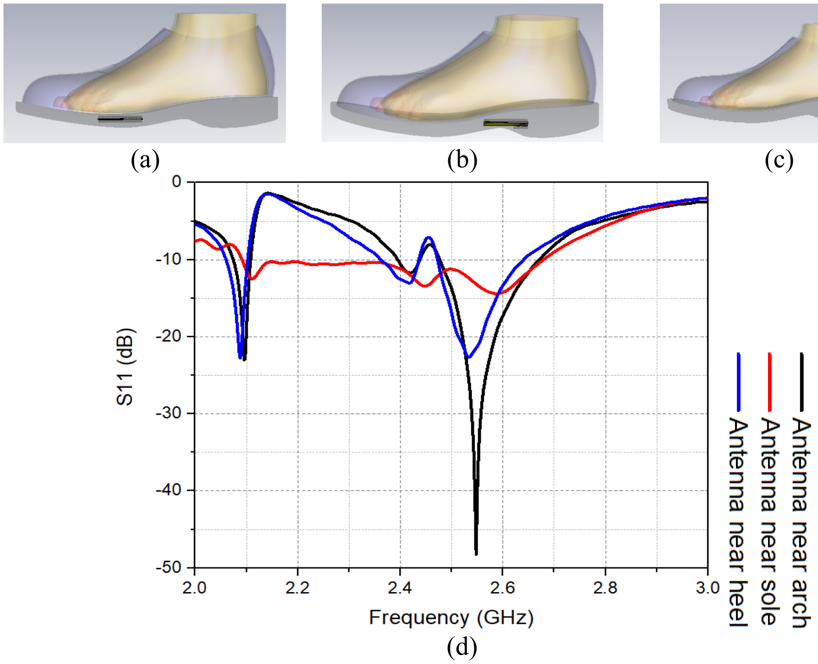

Fig. 6. The position in which the BLE sensor with integrated antenna is placed, a) near the sole, b) near the arch, c) near the heel, d) the simulated S_{11} of the antenna in 3 positions: the green line for near the sole, the blue line for near the arch, the red line for near the heel. (Color figure online)

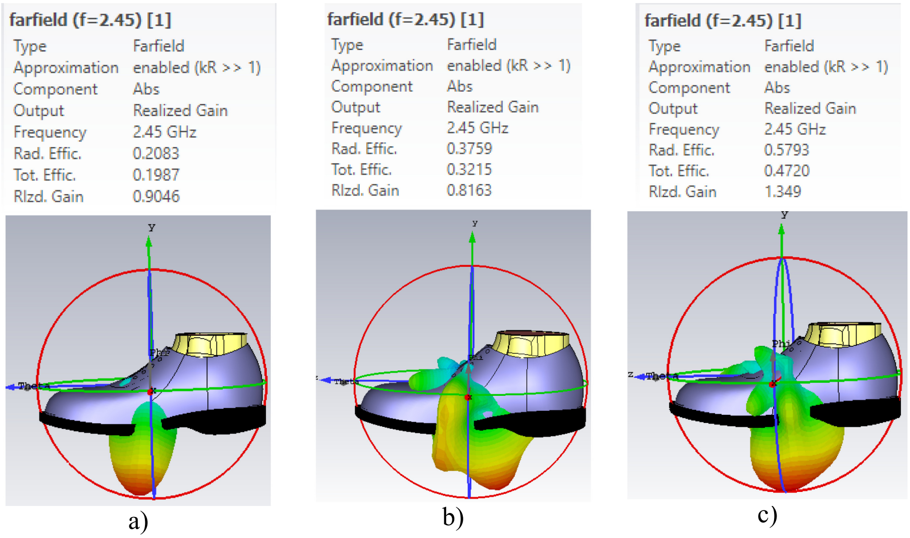

Fig. 7. The radiation patterns of the antenna on BLE sensor node corresponding with 3 position in shoes: a) near the sole, b) near the arch, c) near the heel

2.3 The Proposed Triboelectric Energy Harvester

The mechanical to electrical efficiency must be optimized to harvest energy from the runner footsteps. Due to the up-and-down motion of the foot, the harvester must consist of electrodes which contact to each other vertically. The structure is depicted in Fig. 8:

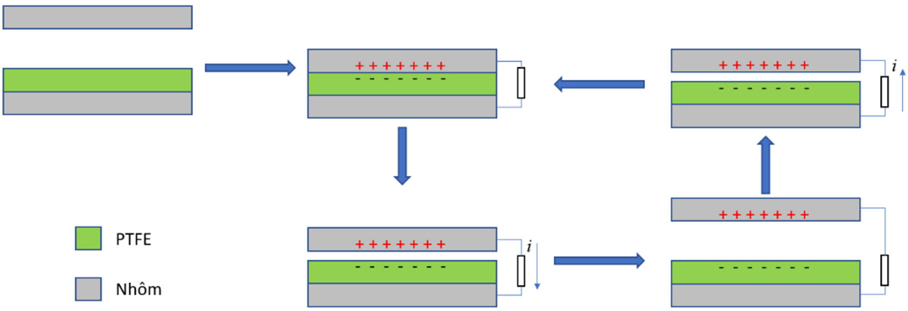

Fig. 8. Structure and operating principle of the triboelectric harvester.

To determine the energy generated by triboelectricity, the charge induced each time the pair of materials get into contact. The area of contact between the layers of PTFE and aluminum play a crucial role, determining how much charge are generated. This area A_r can be calculated from the applied force F, relative coefficient of friction between the two surfaces m_2, and elasticity coefficient E as follow [3]:

$$A_r = \frac{F}{E}\sqrt{\frac{\pi}{m_2}} \tag{1}$$

The relation between A_r and the amount of charge q generated is deduced from [3] as:

$$q = \frac{(\Phi_2 - \Phi_1)\varepsilon_0}{3ex_0} A_r \tag{2}$$

where x_0 is the distance between two surfaces, e is the charge of an electron, Φ_i is the operating state of the two materials, and ε_0 is the permittivity of free space.

After the two surfaces collide, a voltage V_{OC} appears. The PTFE and aluminum layers form a capacitor, with the dielectric insulator consists the air gap of thickness *x(t)* and the PTFE gap of thickness d_2 and permittivity ε_{r2}. V_{OC} is determined as follow:

$$V_{oc} = -\frac{Q}{S\varepsilon_0}\left(\frac{d_2}{\varepsilon_{r2}} + x(t)\right) + \frac{\sigma x(t)}{\varepsilon_0} \tag{3}$$

where Q is the charge already station in the two metallic electrodes, and σ is the charge density induced by triboelectricity.

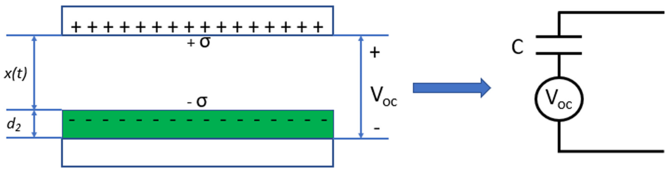

Fig. 9. Equivalent circuit of the TENG.

From the working principle explained above, a multilayer TENG, made of four stacked PTFE and aluminum layers is designed and the equivalent circuit of the TENG is presented in Fig. 9. The IC LTC3331 is employed for power management. Furthermore, the LTC3331 can switch between the TENG and battery, helps both sustain the sensor node, lengthen the using time before having to replace the battery and maintain a stable operation.

3 Device Testing

As seen in Fig. 10, the single layer TENG can harvests 11.26 µW and generates up to 30 V. Meanwhile, for the four layers TENG, these values are respectively 80 V and 80 µW, correspond with 12 µJ per footstep. The output voltage with 10 MΩ load of the single layer and four layers TENG are presented in Fig. 10 b and Fig. 11 b, the period of output voltage for the single layer and four layers TENG are shown in Fig. 10 c and Fig. 11 c. The four layers TENG is employed for the smart shoe as the output voltage is stable and potential to supply for BLE sensor node. The proposed energy harvester is compared to related works in Table 5.

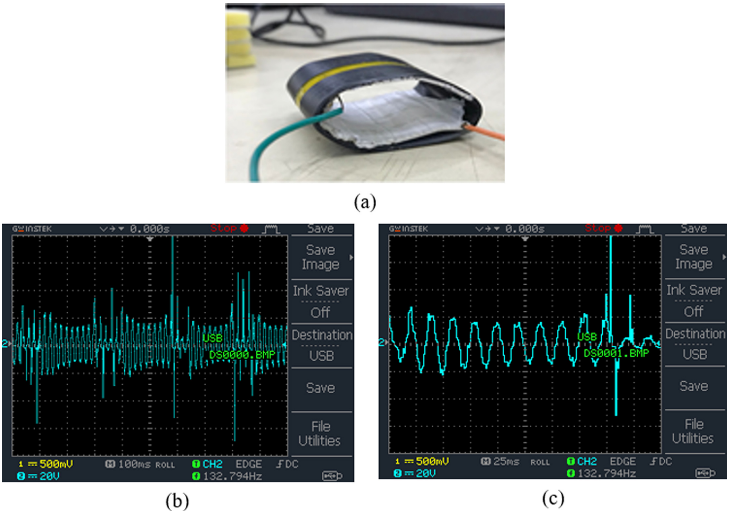

Fig. 10. (a) The single layer TENG, (b) the output voltage with 10 MΩ load, (c) a period of output voltage.

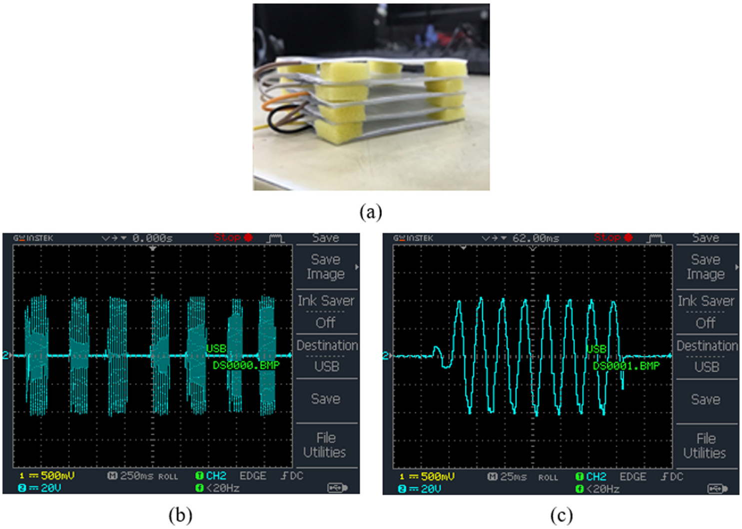

Fig. 11. (a) The multilayer TENG, (b) the output voltage with 10 MΩ load, (c) a period of output voltage.

The triboelectric nanogenerator is connected to the energy storage to power BLE sensor node as in Fig. 12. A comparison between the proposed BLE sensor node and earlier works is listed in Table 6. This work have lower power consumption than the works in [7–9]. At the distance of 10 m between the shoe and the smart phone, 100% measured data is transmited with 0 error showing the potential of the smart shoe.

Table 5. A comparison between the TENG of this work and earlier works.

	[4]	[5]	[6]	This work
Harvested power	19 uW	2294.17 uW	307.88 uW	80 uW
Size	13.1 cm × 9 cm	>5 cm × 5 cm	8 cm × 8 cm	6 cm × 6 cm

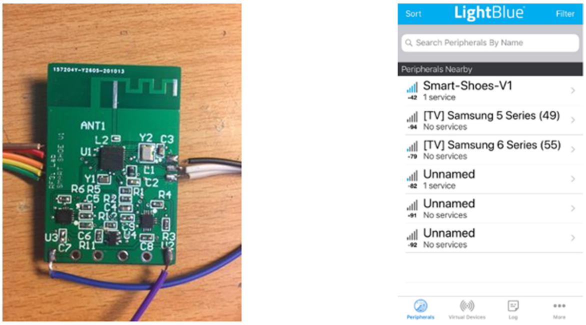

a) b)

Fig. 12. (a) The low-powered sensor node, (b) the application to check the sensor broadcasting package.

Table 6. A comparison between the wireless sensor node of this work and earlier works.

	[7]	[8]	[9]	[10]	This work
Maximum power consumption	33.9 mW	57.09 mW	80 mW	25.37 mW	11.1 mW

4 Conclusion

In this work, idea of a smart shoe based on a wireless sensor node that operates in Bluetooth Low Energy standard, supplied by a triboelectric nanogenerator is investigated and validated. The sensor node consists of an accelerometer and a gyroscope, and consume 11 mW at maximum. The triboelectric nanogenerator harvest up to 32 mW/m^2 with 10 MΩ load, correspond with 12 μJ per footstep. The placed position in the shoe of BLE sensor node is proposed with 10 m of distance of communication withough error.

Acknowledgment. This research is funded by Hanoi University of Science and Technology under grant number T2020-SAHEP-003.

References

1. Wang, Z.L.: Triboelectric nanogenerators as new energy technology for self-powered systems and as active mechanical and chemical sensors. ACS Nano **7**(11), 9533–9557 (2013). https://doi.org/10.1021/nn404614z

2. Datasheet of DA14585, Dialog Semiconductor. https://www.dialog-semiconductor.com
3. Vasandani, P., Mao, Z.-H., Jia, W., Sun, M.: Relationship between triboelectric charge and contact force for two triboelectric layers. J. Electrost. **90**, 147–152 (2017). https://doi.org/10.1016/j.elstat.2017.11.001
4. Shamsuddin, et al.: Biomechanical energy harvesting by single electrode-based triboelectric nanogenerator. In: 2019 2nd International Conference on Computing, Mathematics and Engineering Technologies (iCoMET), Sukkur, Pakistan, pp. 1–5, January 2019. https://doi.org/10.1109/ICOMET.2019.8673493
5. Yingyong, P., Thainiramit, P., Vittayakorn, N., Isarakorn, D.: Performance and behavior analysis of single-electrode triboelectric nanogenerator for energy harvesting floor tiles. In: 2020 17th International Conference on Electrical Engineering/Electronics, Computer, Telecommunications and Information Technology (ECTI-CON), Phuket, Thailand, pp. 514–517, June 2020. https://doi.org/10.1109/ECTI-CON49241.2020.9157902
6. Jurado, U.T., Pu, S.H., White, N.M.: A contact-separation mode triboelectric nanogenerator for ocean wave impact energy harvesting. In: 2017 IEEE SENSORS, Glasgow, pp. 1–3, October 2017. https://doi.org/10.1109/ICSENS.2017.8234198
7. Nair, K., et al.: Optimizing power consumption in iot based wireless sensor networks using Bluetooth Low Energy. In: 2015 International Conference on Green Computing and Internet of Things (ICGCIoT), Greater Noida, Delhi, India, pp. 589–593, October 2015. https://doi.org/10.1109/ICGCIoT.2015.7380533
8. Zagan, I., Găitan, V.G., Petrariu, A.-I., Iuga, N., Brezulianu, A.: Design, fabrication, and testing of an IoT healthcare cardiac monitoring device. Computers **9**(1), 15 (2020). https://doi.org/10.3390/computers9010015
9. Sabatini, A., et al.: Design and development of an innovative sensor system for non-invasive monitoring of athletic performances. In: 2019 II Workshop on Metrology for Industry 4.0 and IoT (MetroInd4.0&IoT), Naples, Italy, pp. 162–166, June 2019. https://doi.org/10.1109/METROI4.2019.8792863
10. Nguyen, N., Nguyen, Q.C., Le, M.T.: A novel autonomous wireless sensor node for IoT applications. TELKOMNIKA (Telecommun. Comput. Electron. Control) **17**(5), 2276–2286 (2019). https://doi.org/10.12928/telkomnika.v17i5.12811